and minimizing γ with respect to d, we obtain the actual width of the interface:

$$d_I/b = [\sum_P \varphi_P{}^b/12\Delta f(0)]^{1/2} \quad \text{(A-12)}$$

and

$$\gamma/\rho_0 b k_B T = b\sum_P \varphi_P{}^b/6d_I \quad \text{(A-13)}$$

For our applications in this paper, it is convenient to express the chemical potential in terms of the asymptotic volume fractions $\varphi_P{}^b$. By noting that for a homogeneous system

$$f = \sum_\kappa \varphi_\kappa \mu_\kappa \quad \text{(A-14)}$$

we see from eq A-2 and A-8 that

$$\Delta f(0) = f|_{x=0} - \tfrac{1}{2}(f|_{x=\infty} + f|_{x=-\infty}) = f\left(\frac{\varphi_A{}^b}{2}, \frac{\varphi_B{}^b}{2}\right) - \frac{1}{2}[f(\varphi_A{}^b,0) + f(0,\varphi_B{}^b)] \quad \text{(A-15)}$$

The results obtained by using eq A-12, A-13, and A-15 agree very well with the more elaborate calculations of our earlier work,[15] as shown in Figure 3. Furthermore, for the case of a nonselective solvent ($\chi_{AS} = \chi_{BS}$), we have

$$\varphi_A{}^b = \varphi_B{}^b = 1 - \varphi_S \quad \text{(A-16)}$$

and hence eq A-12 and A-13 reduce to

$$d_I/b = (2/3\chi_{AB})^{1/2}(1 - \varphi_S)^{-1/2} \quad \text{(A-17)}$$

$$\gamma/\rho_0 b k_B T = (\chi_{AB}/6)^{1/2}(1 - \varphi_S)^{3/2} \quad \text{(A-18)}$$

These results have been derived and used earlier.[15,24]

Registry No. Styrene/butadiene copolymer, 9003-55-8.

References and Notes

(1) Price, C.; Wood, D. *Eur. Polym. J.* **1973**, *9*, 827.
(2) Plestil, J.; Baldrian, J. *Makromol. Chem.* **1975**, *176*, 1009.
(3) Tuzar, Z.; Kratochvil, P. *Adv. Colloid Interface Sci.* **1976**, *6*, 201.
(4) Kotaka, T.; Tanaka, T.; Hattori, M.; Inagaki, H. *Macromolecules* **1978**, *11*, 138.
(5) Stacy, C. J.; Kraus, G. *Polym. Eng. Sci.* **1977**, *17*, 627.
(6) Candau, F.; Guenet, J.-M.; Boutillier, J.; Picot, C. *Polymer* **1979**, *20*, 1227.
(7) Maire, P.; Duplessix, R.; Gallot, Y.; Picot, C. *Macromolecules* **1979**, *12*, 1180.
(8) Marie, P.; Gallot, Y. *Makromol. Chem.* **1979**, *180*, 1611.
(9) Selb, J.; Gallot, Y. *Makromol. Chem.* **1980**, *181*, 809.
(10) Selb, J.; Gallot, Y. *Makromol. Chem.* **1980**, *181*, 2605.
(11) Hong, K. M.; Noolandi, J. *Macromolecules* **1981**, *14*, 727. (A similar approach to the interfacial energy of surfaces with adsorbed polymers has been developed by: Klein, J.; Pincus, P. *Macromolecules* **1982**, *15*, 1129.)
(12) de Gennes, P.-G. "Solid State Physics"; Academic Press: New York, 1978; Suppl. 14, p 1.
(13) Noolandi, J.; Hong, K. M. *Macromolecules* **1982**, *15*, 482.
(14) Flory, P. J. "Principles of Polymer Chemistry"; Cornell University Press: Ithaca, NY, 1953.
(15) Hong, K. M.; Noolandi, J. *Macromolecules* **1981**, *14*, 736.
(16) Brandrup, J.; Immergut, E. G., Eds. "Polymer Handbook"; Interscience: New York, 1966.
(17) Höcker, H.; Blake, G. J.; Flory P. J. *Trans. Faraday Soc.* **1971**, *67*, 2252.
(18) Roe, R.-J.; Zin, W. C. *Macromolecules* **1980**, *13*, 1221.
(19) Dr. Giuseppa DiPaola-Baranyi, Xerox Research Centre of Canada, private communication.
(20) Orwoll, R. A. *Rubber Chem. Technol.* **1977**, *50*, 451.
(21) Inoue, T.; Soen, T.; Hashimoto, T.; Kawai, H. "Block Copolymers"; Aggarwal, S. L., Ed.; Plenum Press: New York, 1970.
(22) de Gennes, P.-G. "Scaling Concepts in Polymer Physics"; Cornell University Press: Ithaca, NY, 1979.
(23) Doi, M.; Edwards, S. F. *J. Chem. Soc., Faraday Trans. 2* **1978**, *74*, 1789.
(24) Helfand, E.; Tagami, Y. *J. Chem. Phys.* **1972**, *56*, 3592.

Effect of Molecular Weight on Polymer Blend Phase Separation Kinetics

Richard Gelles and Curtis W. Frank*

Department of Chemical Engineering, Stanford University, Stanford, California 94305.

Received November 15, 1982

ABSTRACT: The technique of excimer fluorescence has been used to study the effect of molecular weight on the kinetics of phase separation in polystyrene (PS)/poly(vinyl methyl ether) (PVME) blends. From the fluorescence results, which have been analyzed by assuming that demixing occurs by spinodal decomposition, the growth rate of the dominant concentration fluctuation has been determined for 10% and 50% PS blends with PS molecular weights of 100 000 and 1 800 000. At both compositions, the unstable growth rate was found to decrease with increasing PS molecular weight. The observed effect was weaker than expected, presumably due to the polydispersity of the PVME.

Introduction

de Gennes[1] and Pincus[2] have used scaling techniques recently to extend Cahn's theory of spinodal decomposition[3] to polymer blends in the melt. Specifically, their analyses were developed for the case in which both components have the same molecular weight and are above the critical entanglement length. They found two important changes must be made in the theory. First, the dominant term resulting from concentration gradients in the free energy expression is entropic rather than enthalpic. Second, the Onsager coefficient is a function of wavenumber for a given Fourier component of composition because the frictional coefficient describing chain motion in an entangled network depends on the distance scale over which diffusion takes place.

Pincus has shown that the growth rate of the concentration fluctuation which controls the kinetics during the early stages of decomposition is proportional to the melt reptation diffusion coefficient.[2] Thus, provided the thermodynamic driving force for phase separation is kept relatively constant, the kinetics of the early stages of the process should depend strongly on molecular weight. The

0024-9297/83/2216-1448$01.50/0

purpose of this work will be to test this prediction for the blend polystyrene (PS)/poly(vinyl methyl ether) (PVME).

The PS/PVME system has been the subject of numerous fundamental studies because miscible blends exhibiting LCST behavior can be prepared by film casting from toluene.[4-9] More recently, it has been demonstrated that the technique of excimer fluorescence is sensitive to changes in local composition caused by phase separation in this blend. In a study of phase-separated PS/PVME blends prepared by film casting from tetrahydrofuran, a two-phase model was developed to treat quantitatively the fluorescence of phase-separated systems.[10] This two-phase model was subsequently used to analyze the fluorescence from PS/PVME blends phase separated by thermal treatment.[11] In the latter work it was demonstrated that, provided the assumption that the mechanism of phase separation is spinodal decomposition is valid, excimer fluorescence can be used to determine the growth rate of the dominant concentration fluctuation.

The PS/PVME blend is an ideal choice to determine whether the kinetics of spinodal decomposition in polymeric systems is influenced by chain length because polystyrenes of a variety of molecular weights may be readily obtained. However, because this is not the case for PVME, only the effect of varying the PS molecular weight has been examined. Consequently, the work of Pincus and de Gennes has been generalized to blends of polymers of different molecular weights in order to analyze the fluorescence results.

Experimental Section

To ensure that all blend components were above the critical entanglement length of about 200 monomer units,[12] high molecular weight polymers have been used. The polystyrenes, obtained from Pressure Chemical Co., were monodisperse with molecular weights of 100 000 (100K) and 1 800 000 (1800K). The PVME, supplied by GAF, was polydisperse with a molecular weight of 44 600 as determined from its intrinsic viscosity in benzene at 303 K. Although the assumption of an entangled network should hold at all compositions, the spinodal decomposition theory for polymer mixtures was developed by assuming the blend is uniform in composition.[1,2] Because this may not be the case close to the dilute–semidilute crossover point, both 10% and 50% PS blends have been studied. Earlier, it was shown that 10% high molecular weight PS blends are close to this composition since the fluorescence behavior changes little with PS volume fraction below this value.[10]

PS/PVME blends were prepared for spectroscopic study by film casting from toluene onto sapphire disks at room temperature. Purification techniques have been described elsewhere.[13] The solid films, 10 μm thick, were dried under vacuum at 323 K for at least 4 days to remove the casting solvent. No evidence of residual solvent was found in the fluorescence spectra of pure PVME films prepared under identical conditions. To ensure good contact between the films and the cover disk, two of the supported films were pressed together and annealed at 323 K for an additional 2 days. This was found to remove all air spaces in the sample.

Thermal treatment was carried out in an oil bath whose temperature was controlled to ±0.1 K. In order to prevent oil contamination of the samples, they were enclosed in packets formed from the heat-sealable polymer films used in the Dazy Seal-A-Meal cooking pouches. After the sample was held in the bath for the desired annealing time, it was rapidly quenched in an ice–water mixture.

Fluorescence spectra were taken in air at room temperature both before and after thermal treatment. The spectrofluorimeter has been described earlier.[14] Front-face illumination was used to minimize self-absorption; excitation was at 260 nm. The front-face arrangement appeared to reduce self-absorption to a negligible amount, provided the local PS concentration in a blend was not too high. For example, miscible blends do not show a distortion of the monomer bands until the polystyrene volume fraction is greater than 0.8. Of course, the amount of distortion increases with decreasing wavelength. As a result, simple fluorescence intensities were measured at 280 (monomer) and 332 nm (excimer).

Two improvements have been made in the cloud point measurements reported earlier.[11] Previously, glass slides were used as supports for the cloud point samples whereas sapphire disks were used for fluorescence measurements. Because the cloud point temperature has been observed to depend on the substrate,[15] films sandwiched between sapphire disks and prepared in the same manner as fluorescence samples were used in the present work. Second, in the previous paper[11] the cloud point was taken to be the minimum temperature at which a blend showed visual signs of phase separation after 15 min of annealing in the oil bath. In the present study, films were heated starting from 298 K at a rate of 5 K/min; the cloud point was taken to be the temperature at which the first signs of visual opalescence appeared. This method was easier and gave more reproducible results than the technique used previously.

Bright-field transmission optical microscopy was used to examine the morphology of phase-separated films. In order to increase the phase contrast, the aperture diaphragm of the microsope was used in an almost closed position. Unfortunately, this causes both a loss of resolution and shadowing. Film preparation for microscopy was identical with the procedure described above except glass slides and cover slips were used to sandwich the films. Sapphire disks could not be used as film supports in the microscopy work because of the unavailability of long working distance lenses. While this is regrettable, it should be stressed that no quantitative comparison of the microscopy and fluorescence results has been made in the present work.

Spectral Correction Procedure

In the previous study,[11] there was very little overlap of excimer and monomer in the spectra of the phase-separated films examined. This was also true of the spectra of the miscible blends that were needed to analyze the phase-separated film fluorescence with the two-phase model. It should be mentioned that although the high-concentration miscible blend results given in that study do require overlap correction, they were not used in the analysis. In the present paper, however, an overlap correction is needed for both the phase-separated 50% PS blends and the miscible blends required to analyze these fluorescence results. Thus, all ratios of excimer to monomer fluorescence, I_D/I_M, have been corrected for overlap by a procedure described below.

In a separate study, the feasibility of using corrected integrated area fluorescence ratios instead of intensity ratios for PS/PVME blends was determined for miscible 35K PS/PVME blends over the complete concentration range. Fluorescence spectra of these blends were taken with a data acquisition system that has been described earlier.[16] After being corrected for scattered light and instrument response, they were fit to two functional forms. The monomer band was assumed to have the same shape as the fluorescence spectrum of *sec*-butylbenzene dispersed in methanol whereas the excimer was assumed to be Gaussian in shape on an energy scale. While it would have been desirable to determine the shape of the monomer band using a single-ring model compound dispersed in PVME at low concentration, it was rather difficult to prevent low molecular weight species from evaporating out of PVME. From the fits of these spectra, the contribution of excimer fluorescence at 280 nm and monomer fluorescence at 332 nm could be determined.

Representative fitted spectra of 10% and 50% miscible 35K PS/PVME blends are given in Figures 1 and 2. Numerical results showing the contribution of excimer at 280 nm and monomer at 332 nm are given in Table I. It should be noted that this procedure could only be performed for PS volume fractions less than or equal to 0.8

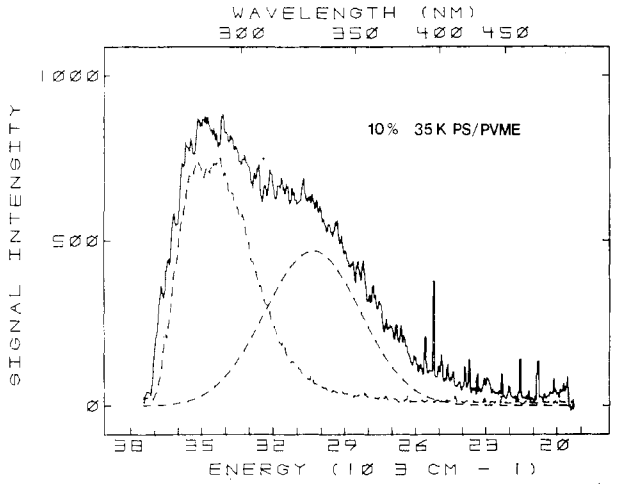

Figure 1. Corrected fluorescence spectrum of 10% 35K PS/PVME blend. The dashed curves show the monomer and excimer bands obtained by fitting the spectrum to the following two functional forms: the monomer band was assumed to have the same shape as the spectrum of *sec*-butylbenzene dispersed in methanol whereas the excimer was assumed to be Gaussian in shape on an energy scale.

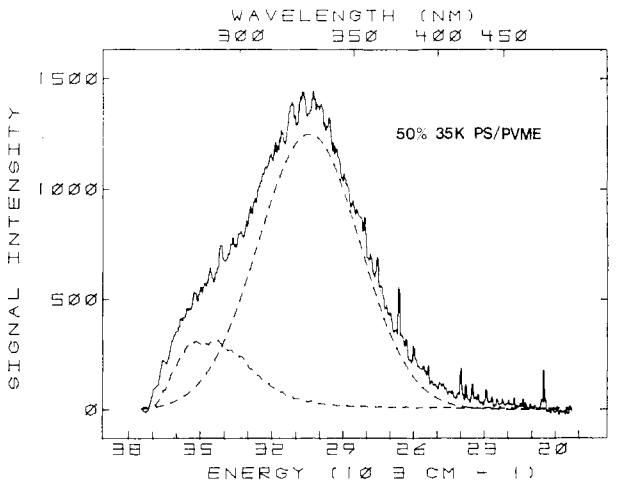

Figure 2. Corrected fluorescence spectrum of 50% 35K PS/PVME blend together with the fitted monomer and excimer bands.

Table I
Overlap Correction Study of 35K Miscible Blends

% PS	uncor int ratio	% excimer contrib at 280 nm	% monomer contrib at 332 nm	cor int ratio
5	0.72	4.8	12.3	0.66
10	0.88	5.5	8.0	0.86
20	1.45	5.6	8.5	1.41
30	2.00	11.3	3.9	2.17
40	2.75	13.0	3.7	3.04
50	3.68	12.3	3.1	4.07
60	4.14	15.6	2.4	4.79
70	5.04	19.5	1.4	6.17
80	6.79	25.4	1.1	9.00
90	9.83	33.0[a]	0.8[a]	14.58
100	12.58	42.0[a]	0.6[a]	21.56

[a] Extrapolated values from Figure 3.

due to self-absorption, which distorts the monomer band at high energies and leads to an artificially high excimer signal.

The results given in Table I can be used to create a calibration curve relating uncorrected intensity ratios to corrected intensity ratios. Such a curve can be used to correct the raw data for any film provided the excimer band position and breadth are invariant. Within experimental error, this was the case for all miscible blends over the entire concentration range and all phase-separated films examined. The excimer was found to be centered at 30 440 ± 190 cm^{-1} with a σ value equal to 2020 ± 170 cm^{-1}, where σ^2 is the variance of the excimer Gaussian. Thus, the correction procedure developed for 35K PS/PVME blends should apply also to the 100K and 1800K blends.

Since the results given in Table I do not cover the complete range of possible fluorescence ratios, they had to be extrapolated. This was accomplished with Figure 3, in which the band overlap contributions have been plotted vs. PS volume fraction and extrapolated over the complete concentration range. The results of the extrapolation are given in Table I. The calibration curve, which relates uncorrected intensity ratios to intensity ratios

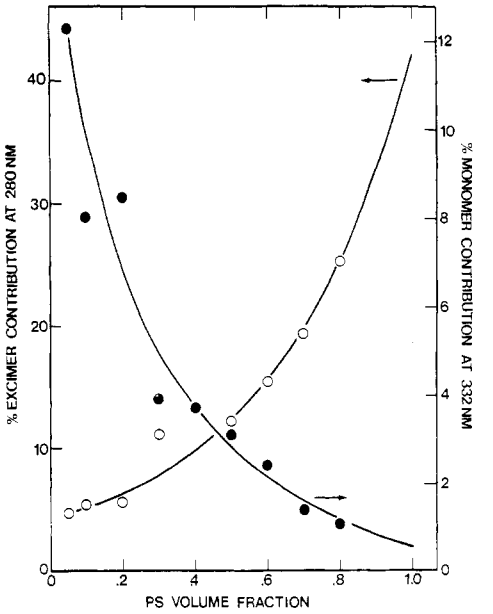

Figure 3. Excimer contribution at 280 nm (○) and monomer contribution at 332 nm (●). The curves have been extrapolated to 100% PS.

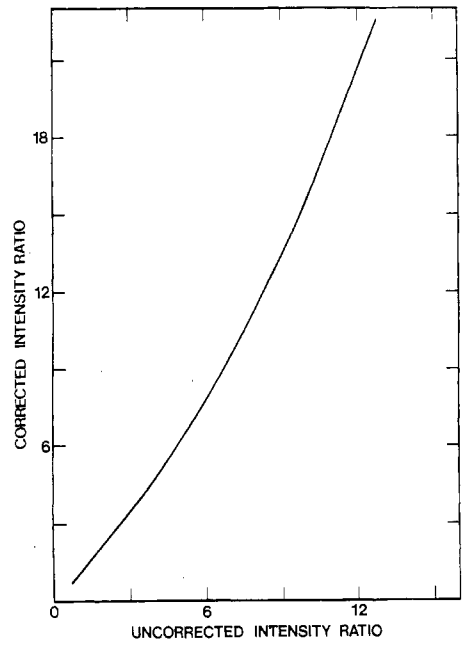

Figure 4. Calibration curve used to correct fluorescence intensity ratios for excimer–monomer overlap.

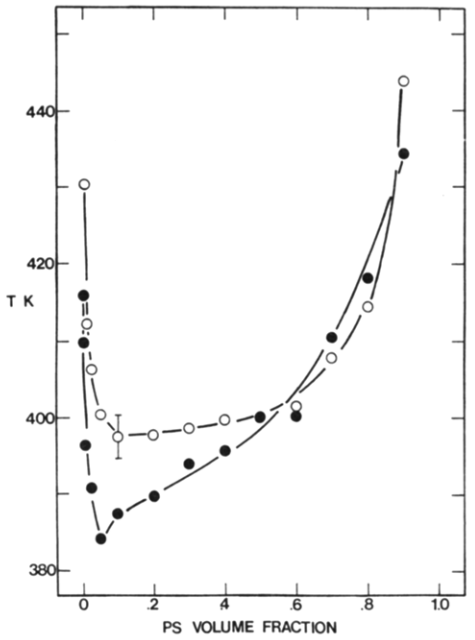

Figure 5. Cloud point curves for 100K (○) and 1800K (●) PS/PVME blends.

corrected for excimer–monomer overlap, is shown in Figure 4.

Results

Cloud point curves for the PS/PVME blends are shown in Figure 5. A similar reversal of the dependence of the cloud point on degree of polymerization for high molecular weight polystyrenes at high PS concentrations has been observed by Nishi and Kwei.[8] In the following analysis it will be assumed for simplicity that these curves represent true binodals, although this assumption is not expected to be strictly valid due to the polydispersity of the PVME.[6,17,18]

To increase the likelihood that the mechanism of phase separation for the 10% and 50% films studied by microscopy and fluorescence was spinodal decomposition, rather than nucleation and growth, an annealing temperature of 423 K, well above the cloud point, was chosen. Some of the microscopy results for blends with 100K PS are shown in Figures 6 and 7. An interconnected morphology was never observed for a 10% film. While it is possible that nucleation and growth take place at this composition and temperature, a more reasonable explanation is that the PS-rich phase does not have a large enough volume fraction to allow connectivity. Cahn has shown that if the minor phase has a volume fraction less than or equal to 0.15, it will exist as disperse particles.[3] From a mass balance together with the cloud point curve, the volume fraction of the rich phase in this blend is calculated to be 0.11. Figure 6 shows that coalescence of the disperse phase droplets takes place with time in the phase-separated 10% 100K PS blend. At 2, 5, and 60 min, the diameters of the particles are of the order 0.6, 1.3, and 6.0 μm, respectively.

Although the characteristic spinodal morphology is present at short times for the 50% 100K PS blend, in Figure 7, an interconnected phase structure in no way proves that the mechanism of phase separation is spinodal decomposition.[3] The size of the phase spacing for the 50% 100K PS blend annealed for 10 min is found from Figure 7a to be about 0.7 μm. At longer times, the interconnected

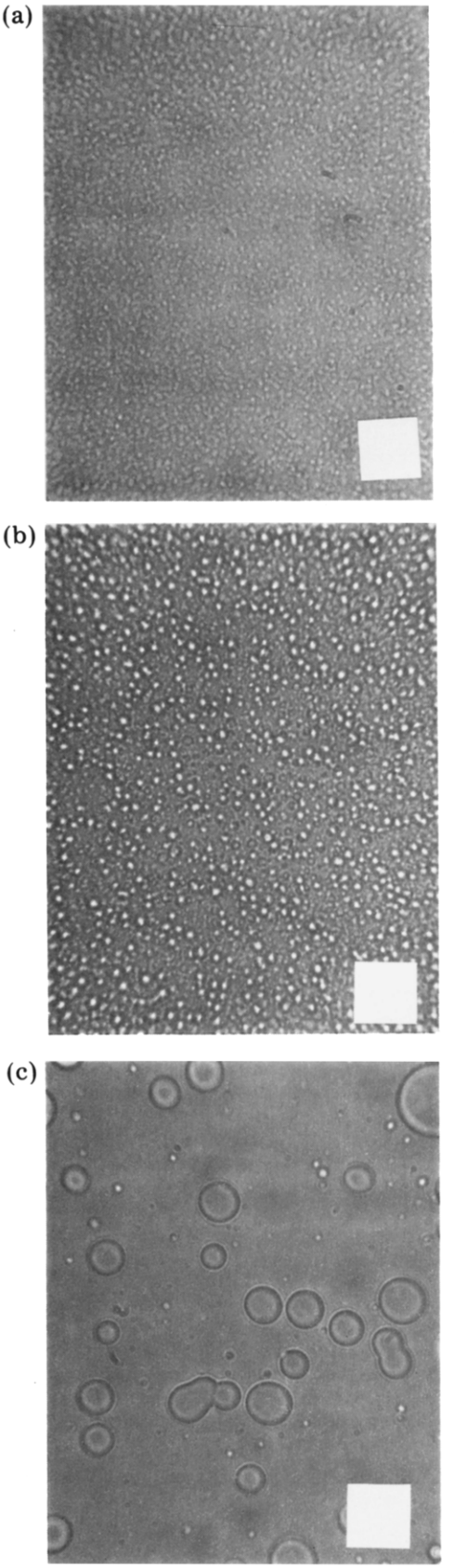

Figure 6. Morphology of 10% 100K PS/PVME blends annealed at 423 K for the times shown. The length of the side of the white square in the photographs corresponds to 10 μm. (a) 2 min; (b) 5 min; (c) 60 min.

structure breaks up into droplets, which then coalesce. By 60 min, the droplet diameter is of the order 4.0 μm. The

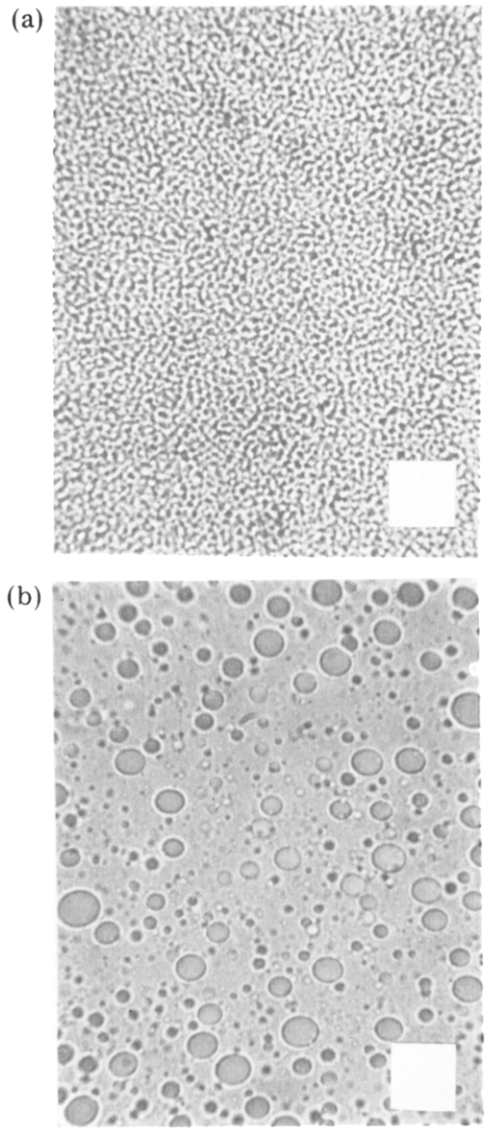

Figure 7. Morphology of 50% 100K PS/PVME blends annealed at 423 K for the times shown. The length of the side of the white square in the photographs corresponds to 10 μm. (a) 10 min; (b) 60 min.

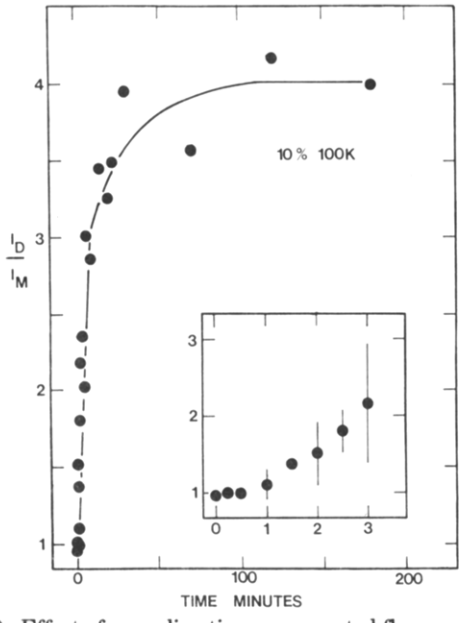

Figure 8. Effect of annealing time on corrected fluorescence ratio for 10% 100K blend annealed at 423 K.

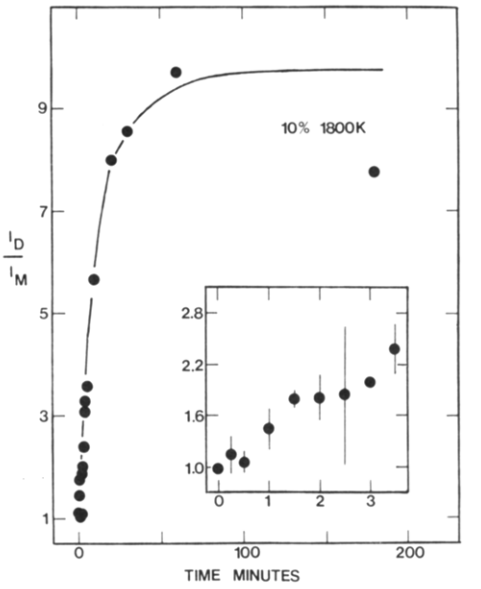

Figure 9. Effect of annealing time on corrected fluorescence ratio for 10% 1800K blend annealed at 423 K.

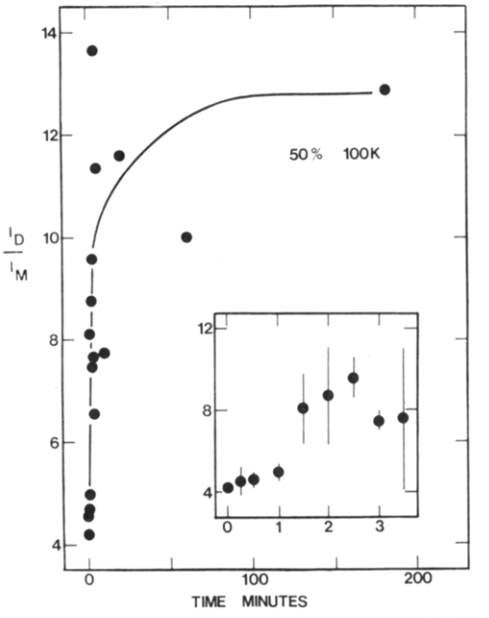

Figure 10. Effect of annealing time on corrected fluorescence ratio for 50% 100K blend annealed at 423 K.

coalescence of both disperse and interconnected phase structures in polymer blends has been studied by McMaster.[19]

Optical microscopy could not be used to examine films that were annealed for very short times. In fact, two phases could be discerned under magnification only when the sample appeared cloudy to the naked eye. The time required for opalescence to first appear varied from blend to blend but was approximately 1 min in all cases.

The dependence of the corrected intensity ratio of excimer to monomer fluorescence, I_D/I_M, on time of annealing at 423 K for the four blends studied is shown in Figures 8–11. Uncorrected fluorescence spectra of 10% 100K PS blends annealed for different times have been shown previously. The ratios at $t = 0$ are average ratios for films bfore thermal treatment. For each blend, I_D/I_M increases rapidly with time during the first 10 min. At longer times, it appears that a much slower change may be occurring, although the scatter in the data makes it difficult to reach a conclusion.

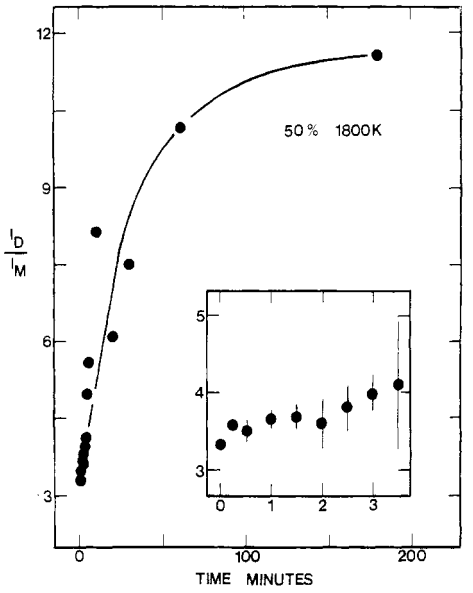

Figure 11. Effect of annealing time on corrected fluorescence ratio for 50% 1800K blend annealed at 423 K.

Table II
Phase Diagram Information

% PS	PS MW	ϕ_R binodal	ϕ_L binodal	$T_{cloud\ point}$, K
10	100K	0.845	0.007	398
50	100K	0.845	0.007	399
10	1800K	0.825	<0.001	388
50	1800K	0.825	<0.001	398

It is of interest to make a qualitative comparison of the microscopic and fluorescence results. The sensitivity of the fluorescence probe to the early stages of phase separation is illustrated by the fact that films annealed for about 1 min showed no visual signs of opalescence and no phase structure under magnification while I_D/I_M increased between 10% and 49% for the different blends examined. It is apparent from these observations that much of the compositional change during the phase separation process takes place long before a discernible morphology can be observed by optical means.

Discussion

Because the fluorescence studies show that changes in phase composition take place before a discernible morphology can be observed by optical microscopy, only the fluorescence results will be used to examine the early stage of the phase separation process.

The two-phase model used to analyze the fluorescence of phase-separated films has been discussed in detail previously[10,11] and will not be presented here. If phase separation is taking place by spinodal decomposition, then the volume fraction of each phase will remain constant. As a result, the two-phase model can be used to determine the dependence of the rich- and lean-phase compositions with time provided the binodal concentrations are known. In Table II, the required information from the phase diagrams is given.

Figures 12 and 13 show the dependence of the rich-phase polystyrene concentration ϕ_R with time for each of the four blends. Only short-time results are depicted since very little change in phase composition takes place after 5 min in all cases. In Table III, results for the complete time interval examined are given.

For a blend of two polymers with the same molecular weight, the time dependence of the early stages of the

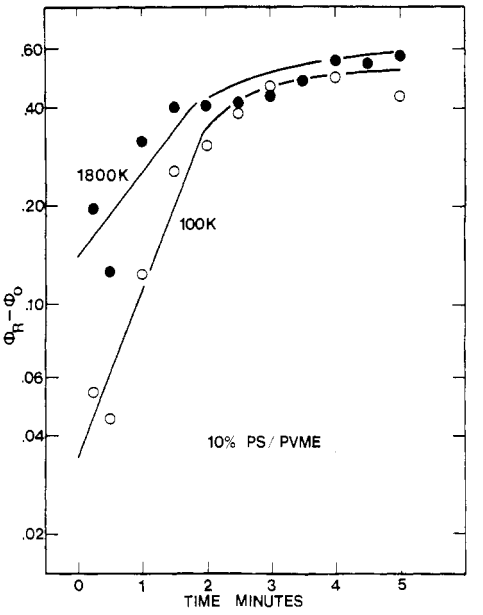

Figure 12. Change in the rich-phase composition with annealing time for 10% PS blends.

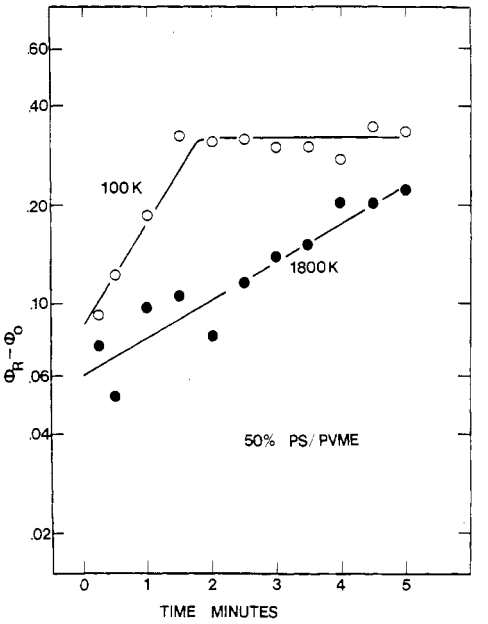

Figure 13. Change in the rich-phase composition with annealing time for 50% PS blends.

phase separation process is governed by the modified diffusion equation[1]

$$\frac{\partial\phi}{\partial t} = \Lambda\left\{\left[\frac{1}{N\phi(1-\phi)} - 2\chi\right]\nabla^2\phi - \frac{a^2}{36\phi(1-\phi)}\nabla^4\phi\right\} \quad (1)$$

where ϕ is the volume fraction of one of the components, t is time, Λ is the Onsager coefficient, defined as the ratio of the diffusional flux to the chemical potential gradient, N is the number of monomer units in the chain, χ is an interaction parameter, and a is a typical monomer dimension.

The solution to eq 1 is a Fourier series that can be approximated by its maximum term[3]

$$\phi - \phi_0 = \exp[-t/\tau_{q_{max}}] \sum_{|\mathbf{q}|=q_{max}} [A(\mathbf{q}) \cos(\mathbf{q}\cdot\mathbf{r}) + B(\mathbf{q}) \sin(\mathbf{q}\cdot\mathbf{r})] \quad (2)$$

where ϕ_0 is the initial composition, $\mathbf{q}$ is a wave vector, A and B are amplitudes, and $\mathbf{r}$ is position. Finally, $\tau_{q_{max}}^{-1}$

Table III
Two-Phase Model Results

time, min	$\phi_R - \phi_0$ 10% 100K	10% 1800K	50% 100K	50% 1800K
0.25	0.054	0.196	0.093	0.074
0.5	0.045	0.126	0.124	0.052
1.0	0.125	0.317	0.187	0.097
1.5	0.257	0.401	0.325	0.106
2.0	0.309	0.405	0.311	0.080
2.5	0.388	0.413	0.319	0.116
3.0	0.463	0.438	0.301	0.140
3.5		0.487	0.301	0.152
4.0	0.493	0.556	0.273	0.204
4.5		0.545	0.345[a]	0.204
5.0	0.433	0.572	0.335	0.224
7.0	0.551			
10.0	0.548	0.640	0.302	0.270
15.0	0.598			
20.0	0.583	0.673	0.337	0.239
23.0	0.601			
30.0	0.628	0.679	0.345[a]	0.262
60.0		0.693	0.323	0.294
71.0	0.606			
120.0	0.641			
180.0	0.631	0.670	0.345[a]	0.304

[a] Observed ratio was larger than the maximum possible ratio predicted by two-phase model; ϕ_R taken to be ϕ_R(equilibrium).

Table IV
Growth Rate

% PS	PS MW	time interval over which slope obtained,[a] min	$-\tau_{q_{max}}^{-1}$, min^{-1}
10	100K	2.0	1.18
10	1800K	2.0	0.60
50	100K	2.0	0.74
50	1800K	5.0	0.27

[a] The slopes were obtained by a linear least-squares regression.

is the growth rate of concentration fluctuations with wavenumber q_{max}, which are the Fourier components with the maximum growth rate. The growth rate depends on wavenumber as follows:[1]

$$-\tau_q^{-1} = \Lambda(q)q^2\left[2\chi - \frac{1}{N\phi(1-\phi)} - \frac{(aq)^2}{36\phi(1-\phi)}\right] \quad (3)$$

From eq 2, which also holds for the unsymmetrical molecular weight case, it is apparent that the growth rate of the dominant concentration fluctuation can be obtained from the linear portion of the curves in Figures 12 and 13. These results are given in Table IV.

For a blend of two polymers with the same molecular weight, Pincus[2] determined that the Onsager coefficient is given by

$$\Lambda(q) = \phi(1-\phi)2T\mu_0(qL)^{-2}[1 - \exp(-q^2R_0^2/6)] \quad (4)$$

Here, μ_0 is a microscopic mobility assumed to be the same for both components, R_0^2 is the mean squared end-to-end distance of a chain, equal to Na^2, T is the temperature, and L is the length of the tube formed by the entangled network in which the monomers of a chain are confined. The tube length is related to the average number of monomer units between entanglements N_e

$$L \sim NN_e^{-1/2}a \quad (5)$$

From eq 3 and 4 together with the assumption that $q_{max}^2R_0^2/6 < 1$, Pincus found[2]

$$q_{max}^{-1} \sim R_0(\chi/\chi_s - 1)^{-1/2} \quad (6)$$

and

$$-\tau_{q_{max}}^{-1} \sim \frac{T\mu_0N_e}{a^2}\phi(1-\phi)\frac{(\chi-\chi_s)^2}{\chi_s}\frac{1}{N^2} \quad (7)$$

Before the experimental results can be discussed, the theory of de Gennes and Pincus must be extended to blends with different molecular weight components. It is worthwhile to point out before proceeding, however, that due to the difference in the glass transition temperatures of the two components, monomer mobility is expected to change with blend composition. As a result, only the variation in the growth rate with change in PS molecular weight at fixed initial composition will be addressed here.

In the small-wavenumber limit, de Gennes[1] has shown that the assumption of incompressibility leads to a simple relation between the Onsager coefficients of each component and the overall one

$$\Lambda = \Lambda_A\Lambda_B/(\Lambda_A + \Lambda_B) \quad (8)$$

where $\Lambda_i = D_iN_i\phi_i$ and D_i is the macroscopic or reptation diffusion coefficient. For $q = 0$, it must be true that

$$ND_{rep} = N_eD_{tube} \quad (9)$$

where D_{tube} is the diffusion coefficient describing motion of a chain along its tube. Equation 8 may be written for general q by using the usual scaling approach

$$\Lambda(q) = \frac{N_e\phi_A\phi_BD_{tube\ A}(q)D_{tube\ B}(q)}{D_{tube\ A}(q)\phi_A + D_{tube\ B}(q)\phi_B} \quad (10)$$

In eq 10, N_e has been assumed to be the same for both components. This may done by taking the typical monomer dimension to be the size of the smaller of the two monomer units, dividing the other component's chains up accordingly, and assuming that entanglement properties only depend on repeat unit size. Upon making this assumption, it is apparent that the Pincus expression for the tube diffusion coefficient[2] still holds

$$D_{tube\ i}(q) = \frac{2T\mu_0}{N_e}(qL_i)^{-2}[1 - \exp(-q^2R_{0i}^2/6)] \quad (11)$$

where it has been assumed that the monomer mobility is the same for both species. (The factor N_e^{-1} appears to have been misplaced in the original expresion.[2])

The modified diffusion equation for the unsymmetrical molecular weight case is

$$\frac{\partial\phi}{\partial t} = \Lambda\left\{\left[\frac{1}{N_A\phi_A} + \frac{1}{N_B(1-\phi_A)} - 2\chi\right]\nabla^2\phi - \frac{a^2}{36\phi_A(1-\phi_A)}\nabla^4\phi\right\} \quad (12)$$

The solution of the above equation may be approximated by eq 2, where

$$-\tau_q^{-1} = \Lambda(q)q^2\left[2\chi - \left(\frac{1}{N_A\phi_A} + \frac{1}{N_B(1-\phi_A)}\right) - \frac{(aq)^2}{36\phi_A(1-\phi_A)}\right] \quad (13)$$

Equations 10, 11, and 13 and the assumptions that

$$q^2R_{0A}^2/6 < 1$$

and

$$q^2R_{0B}^2/6 < 1$$

lead to the following scaling relationships:

$$q_{max}^{-1} \sim \frac{R_{0A}R_{0B}}{(R_{0A}^2\phi_A + R_{0B}^2\phi_B)^{1/2}}\left(\frac{\chi}{\chi_s} - 1\right)^{-1/2} \quad (14)$$

and

$$-\tau_{q_{max}}^{-1} \sim \frac{T\mu_0 N_e}{a^2}\phi_A(1-\phi_A)\frac{(\chi-\chi_s)^2}{\chi_s}\frac{1}{N_AN_B}\frac{\phi_AN_A + \phi_BN_B}{\phi_AN_B + \phi_BN_A} \quad (15)$$

where χ_s is the interaction parameter evaluated at the spinodal given by

$$2\chi_s = \frac{1}{N_A\phi_A} + \frac{1}{N_B\phi_B} \quad (16)$$

For fixed initial composition and annealing temperature, eq 15 may be simplified to

$$-\tau_{q_{max}}^{-1} \sim \frac{(\chi-\chi_s)^2}{\chi_s}\frac{1}{N_AN_B}\frac{\phi_AN_A + \phi_BN_B}{\phi_AN_B + \phi_BN_A} \quad (17)$$

The Flory–Huggins free energy expression will not work for a blend exhibiting a LCST unless it is assumed that the interaction parameter depends on temperature. The appropriate temperature dependence required is[20]

$$\chi = A - B/T \quad (18)$$

which should be a reasonable approximation over a limited temperature range. Thus

$$-\tau_{q_{max}}^{-1} \sim \frac{1}{\phi_AN_B + \phi_BN_A}\left(\frac{T-T_s}{T_s}\right)^2 \quad (19)$$

In order to use eq 19, molecular weight will be defined relative to the size of a PVME repeat unit. In other words

$$N_i = \frac{M_i}{M_i^0}\frac{V_i^0}{V_{PVME}^0}$$

$$V_i^0 = M_i^0/\rho_i \quad (20)$$

where M_i is the molecular weight of component i, M_i^0 and V_i^0 are the molecular weight and molar volume, respectively, of a repeat unit of species i, and ρ_i is the density of species i. Of course, the density and volume fraction of each component must be determined at the annealing temperature. The density of PS at 423 K can be determined from its value at 298 K together with thermal expansion coefficient data. This information is given in Table V along with the calculated value of the density at 423 K. Since thermal expansion coefficient data could not be found for PVME, the value given in Table V was calculated according to the empirical rule[23]

$$\alpha_l = 0.16/T_g \quad (21)$$

where α_l is the thermal expansion coefficient and T_g is the glass transition temperature. The glass transition temperature of PVME is approximately 245 K.[4] From eq 20 together with the density values at 423 K, the following degrees of polymerization are obtained: $N_{PVME} = 769$, $N_{100K\ PS} = 1650$, and $N_{1800K\ PS} = 29\,800$.

Before eq 19 is used to predict how the growth rate of the dominant concentration fluctuation depends on PS molecular weight, the volume fractions of each component must be calculated at 423 K. This may be done by using the relationship

$$\phi_{PS\ 423\ K} = \frac{\phi_{PS\ 298\ K}/\rho_{PS\ 423\ K}}{\phi_{PS\ 298\ K}/\rho_{PS\ 423\ K} + \phi_{PVME\ 298\ K}/\rho_{PVME\ 423\ K}} \quad (22)$$

For the 50/50 blend, $\phi_{PS\ 423\ K} = 0.49$ while for the 10/90 blend, $\phi_{PS\ 423\ K} = 0.096$.

Finally, because the value of T_s is not known for the blends studied, the cloud point temperatures given in Table II will be used in eq 19. A comparison of the observed and predicted molecular weight dependence of the growth rate is made in Table VI.

Provided the thermodynamic driving force for phase separation is relatively constant, eq 19 predicts that the growth rate of the dominant concentration fluctuation should decrease as the PS molecular weight increases. While this is observed qualitatively, a weaker effect than predicted is found at both compositions examined. In addition, the deviations of the observed growth rates from those predicted by the modified scaling arguments are essentially identical for both initial concentrations, despite the fact that the 10% blends may be too close to the semidilute–dilute crossover composition for the assumption of initial uniformity to apply.

The numerous assumptions made in developing and applying the spinodal decomposition theory already discussed above need not be repeated here. There is an additional problem in the analysis which has been ignored, however, and which is perhaps the single most important cause of the difference between the theoretical predictions and the experimental observations. This problem is the neglect of the PVME polydispersity. In addition to having PVME chains with a wide range of frictional coefficients, the presence of short unentangled chains that can diffuse rapidly during the early stages of phase separation is expected to weaken the molecular weight dependence of the growth rate. However, since this effect should become less important as the PS concentration is increased, which has not been observed, there does seem to be quantitative disagreement with theory and experiment on the molecular weight dependence of the growth rate.

Table V
Density and Thermal Expansion Coefficient Data

polymer	$\rho_{298\ K}$, g/cm^3	thermal expansion coeff, K^{-1}	$\rho_{423\ K}$, g/cm^3
PS	1.04[a]	$(1.7\text{-}2.1) \times 10^{-4}$ K^{-1}, $T < 373$ K[b] $(5.1\text{-}6.0) \times 10^{-4}$ K^{-1}, $T > 373$ K[b]	1.00
PVME	1.04[a]	6.53×10^{-4} K^{-1}[c]	0.96

[a] From ref 21. [b] From ref 22. [c] Calculated from eq 21.

Table VI
Observed and Predicted Dependence of the Growth Rate on PS Molecular Weight

	$(-\tau_{q_{max}})^{-1}_{100K\ PS}/(-\tau_{q_{max}})^{-1}_{1800K\ PS}$		
% PS	obsd	pred	pred/obsd
10	1.97	8.60	4.4
50	2.74	11.77	4.3

Summary

The growth rate of the dominant concentration fluctuation during the initial stages of spinodal decomposition in PS/PVME blends has been found to decrease with increasing PS molecular weight. This effect, which is

predicted by scaling theory, was weaker than expected. A possible explanation is that short unentangled PVME chains in the polydisperse PVME used in this study, strongly affect the kinetics of the early stages of the process due to their high mobility.

Acknowledgment. This work was supported by the Army Research Office under Contracts DAAG 29-78-C-0047 and DAAG 29-82-K-0019.

Registry No. Polystyrene, 9003-53-6; poly(vinyl methyl ether), 9003-09-2.

References and Notes

(1) de Gennes, P.-G. *J. Chem. Phys.* **1980**, *72*, 4756.
(2) Pincus, P. *J. Chem. Phys.* **1981**, *75*, 1996.
(3) Cahn, J. W. *J. Chem. Phys.* **1965**, *42*, 93.
(4) Bank, M.; Leffingwell, J.; Thies, C. *Macromolecules* **1971**, *4*, 43.
(5) Bank, M.; Leffingwell, J.; Thies, C. *J. Polym. Sci., Part A-2* **1972**, *10*, 1097.
(6) McMaster, L. P. *Macromolecules* **1973**, *6*, 760.
(7) Kwei, T. K.; Nishi, T.; Roberts, R. F. *Macromolecules* **1974**, *7*, 667.
(8) Nishi, T.; Kwei, T. K. *Polymer* **1975**, *16*, 285.
(9) Nishi, T.; Wang, T. T.; Kwei, T. K. *Macromolecules* **1975**, *8*, 227.
(10) Gelles, R.; Frank, C. W. *Macromolecules* **1982**, *15*, 747.
(11) Gelles, R.; Frank, C. W. *Macromolecules* **1982**, *15*, 1486.
(12) de Gennes, P.-G. "Scaling Concepts in Polymer Physics"; Cornell University Press: Ithaca, NY, 1979.
(13) Gelles, R.; Frank, C. W. *Macromolecules* **1982**, *15*, 741.
(14) Frank, C. W.; Gashgari, M. A. *Macromolecules* **1979**, *12*, 163.
(15) Reich, S.; Cohen, Y. *J. Polym. Sci., Polym. Phys. Ed.* **1981**, *19*, 1255.
(16) Fitzgibbon, P. D.; Frank, C. W. *Macromolecules* **1981**, *14*, 1650.
(17) Koningsveld, R.; Staverman, H. J. *Kolloid-Z. Z. Polym.* **1967**, *218*, 114.
(18) Koningsveld, R.; Staverman, A. J. *J. Polym. Sci., Part C* **1967**, *16*, 1775.
(19) McMaster, L. P. *Adv. Chem. Ser.* **1975**, *No. 142*, 43.
(20) Koningsveld, R.; Kleintjens, L. A. *J. Polym. Sci., Polym. Symp.* **1977**, *No. 61*, 221.
(21) Lewis, O. G. "Physical Constants of Linear Homopolymers"; Springer-Verlag: New York, 1968.
(22) Brandrup, J.; Immergut, E. H., Eds. "Polymer Handbook"; Wiley: New York, 1975.
(23) Van Krevelen, D. W. "Properties of Polymers"; Elsevier: New York, 1976.

Electronic Excited-State Transport on Isolated Polymer Chains

Glenn H. Fredrickson, Hans C. Andersen,* and Curtis W. Frank

Departments of Chemical Engineering and Chemistry, Stanford University, Stanford, California 94305. *Received February 1, 1983*

ABSTRACT: A theory for the incoherent transport of electronic excitations among chromophores on a polymer chain is presented. The approach is general, but calculations are performed for the special case of Förster transfer on an ideal chain. The chain is assumed to contain a small concentration of randomly placed chromophores. A three-dimensional model of intersite transport is developed, and an estimate is made of its region of validity. The model is formulated in terms of a diagrammatic expansion of the Green function solution to the transport master equation. Topological reduction of the diagrammatic series leads to a Dyson equation for the diagonal elements of the Green function that can be used as the basis for a class of self-consistent approximations. The Dyson equation takes a very simple form for infinite chains, and self-consistent calculations for $G^s(t)$, the ensemble-averaged probability of the excitation being on its initial site, are performed for this case. The results are compared with calculations based on Padé approximants and cumulants constructed from a density expansion for $G^s(t)$. A connection is made between $G^s(t)$ and the observables in transient and photostationary fluorescence depolarization experiments, and the importance of proper orientation averaging of transition dipoles is discussed.

I. Introduction

Fluorescence techniques have proven to be quite useful as probes of polymer structure and dynamics.[1,2] Depolarization experiments have been used to determine bulk rotational diffusion constants of macromolecules[3] and also to measure the rate of conformational transitions.[4] The analysis of such experiments is often complicated by the presence of electronic energy transport (EET) between the chromophores of the system. Other experiments, however, rely on EET to provide the structural and dynamical information. By monitoring the ratio of integrated excimer to monomer emission it has been possible to study the thermodynamic compatibility of solid polymer blends[5] and the mechanism of spinodal decomposition in macromolecular systems.[6] Steady-state fluorescence depolarization resulting from resonant energy transfer has also been used extensively to analyze copolymers containing aromatic moieties.[7]

This is the first in a series of papers whose purpose is to explore the use of fluorescence depolarization and related techniques to study the structure of polymeric materials. In this paper we consider the case of an isolated ideal chain. Transient and photostationary fluorescence measurements will be seen to give direct information on chain stiffness and local chromophore density within such a random coil. In subsequent papers, we will extend the present theory to more complicated morphologies, such as interacting chains in solution or in solid blends, and to other experiments such as trap fluorescence studies.

The general many-body problem of incoherent excitation transfer among randomly distributed sites in a homogeneous material has been elegantly formulated by Haan and Zwanzig[8,9] and solved approximately with various types of theoretical methods.[8-12] Few attempts have been made to address the corresponding problem for inhomogeneous materials or for chromophores on polymer chains.[13] The lack of translational symmetry, correlated statistics, and the large chromophore concentrations often encountered in macromolecular systems increase the difficulty of the theoretical analysis.

One of the approximate methods for solving the problem of random sites in a homogeneous material is that of Gochanour, Andersen, and Fayer[10] (hereafter referred to as GAF). It is based on a diagrammatic expansion of the transport Green function. Their formalism leads to a class of self-consistent approximations that converge rapidly and

0024-9297/83/2216-1456$01.50/0